




Cite this: *Mater. Adv.*, 2023,  
4, 5215

# Supramolecular inclusion complexes of $\beta$ -cyclodextrin with bathochromic-shifted photochromism and photomodulable fluorescence enable multiple applications†

Dong-Xue Xia,<sup>a</sup> Li-Wen Fan,<sup>a</sup> Ming-Fu Ye,<sup>ab</sup> Wen-Qi Sun,<sup>\*a</sup> Rui-Lian Lin<sup>a</sup> and  
Jing-Xin Liu  <sup>\*a</sup>

Three distinct viologen derivatives have been designed and successfully synthesized. They have been shown to form 1:1 or 2:1 host–guest inclusion complexes with  $\beta$ -cyclodextrin ( $\beta$ -CD) in aqueous solution. In comparison with the traditional *N*-alkyl-substituted viologen, the inclusion complexes of the conjugation-extended viologens with  $\beta$ -CD exhibit interesting bathochromic-shifted photochromic behaviors in the solid state, which have been characterized by UV-vis diffuse-reflectance and electron-spin resonance (ESR) spectroscopy. Owing to the bathochromic-shift effect, the photoproducts of these three inclusion complexes undergo significant color changes from blue to green and then to orange. In addition, these three inclusion complexes display interesting photomodulable fluorescence emissions. The excellent photochromic and fluorescence properties of these three inclusion complexes endow them with potential applications in protection, erasable inkless multi-color printing, multiple anti-counterfeiting and multilevel information encryption, which have also been extensively demonstrated in this work.

Received 9th August 2023,  
Accepted 19th September 2023

DOI: 10.1039/d3ma00527e

rsc.li/materials-advances

## Introduction

The two typical features of photochromic materials are color changes and absorption spectra alteration when exposed to light, which endow them with important technological applications, such as protection, displays, optical sensors, electronic papers, anti-counterfeiting, and so on.<sup>1–18</sup> Among various organic photochromic families, viologen (1,1'-disubstituted 4,4'-bipyridinium dication) derived photochromic materials are particularly attractive not only because of their excellent thermostability and reversibility, but also because of their photochromic mechanism of photo-induced electron transfer, which does not cause significant geometric change and large volume change during the photochromic process.<sup>19,20</sup> Over the

past decade, a great deal of viologens have been synthesized and used to develop photochromic systems.<sup>20–34</sup> However, promoting the practical application of viologen-based photochromic materials remains a great challenge because the redox process of traditional *N*-alkyl-substituted viologens usually exhibits monotonous color changes between colorless  $V^{2+}$  and blue  $V^{\bullet+}$ .

To obtain other color variations, the  $\pi$ -conjugation length of the viologens should be increased, and two methods have been reported to achieve this target.<sup>35–48</sup> One of the methods is to insert a conjugate group into the two pyridinium groups. For example, Zhou *et al.* incorporated thiophene and its derivatives into viologens.<sup>36</sup> The electrochromic response of the formed thieno-viologens is extended to the near-infrared region. Another method is to connect two conjugating groups from the outside to the two pyridinium groups. For instance, Lin and coworkers very recently synthesized a conjugated viologen of *N,N'*-bis(4-carboxyphenyl)-(4,4'-bipyridinium) dichloride for the development of X-ray-induced photochromic materials.<sup>48</sup> All these reported conjugation-extended viologens clearly possess potential photochromic properties and are excellent constituents for constructing photochromic materials.

Our efforts in constructing photochromic systems have been focused on the use of macrocyclic hosts.<sup>49–55</sup>  $\beta$ -Cyclodextrin ( $\beta$ -CD) is a truncated cone-shaped cyclic oligomer consisting of

<sup>a</sup> College of Chemistry and Chemical Engineering, Anhui University of Technology, Maanshan 243002, China. E-mail: jxliu411@ahut.edu.cn, wengqisun@sohu.com

<sup>b</sup> Anhui Province Key Laboratory of Chemistry for Inorganic/Organic Hybrid Functionalized Materials, Anhui University, Hefei 230601, China

† Electronic supplementary information (ESI) available: 2D gCOSY NMR spectra of the three viologens, <sup>1</sup>H NMR spectra of  $\beta$ -CD with the viologens 1-Cl<sub>2</sub> and 2-Cl<sub>2</sub>, photographs of the surface and internal colors of the inclusion complexes after irradiation, electron distributions on the HOMO and LUMO, FT-IR spectra of the three inclusion complexes before and after irradiation, photomodulable fluorescence of 1<sup>2+</sup>@ $\beta$ -CD and 2<sup>2+</sup>@ $\beta$ -CD<sub>2</sub>, and the customized codebooks. See DOI: <https://doi.org/10.1039/d3ma00527e>



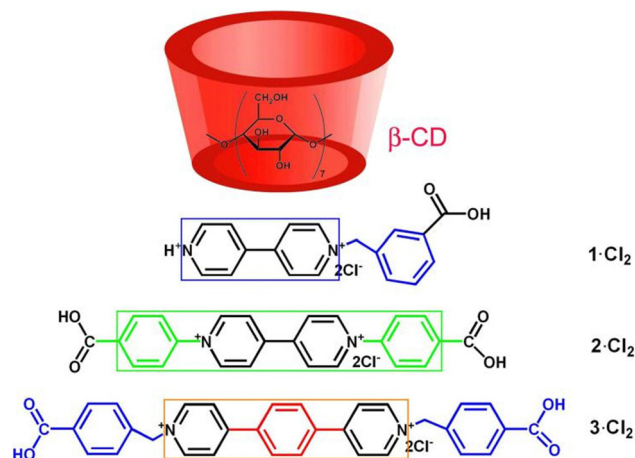


Fig. 1 Structures of the  $\beta$ -CD and the viologens studied in this work. The colored square frames indicate the  $\pi$ -conjugation length of the viologens.

seven D-glucose units.<sup>56–59</sup> As shown in Fig. 1,  $\beta$ -CD possesses two different size portals laced by hydroxyl groups and a hydrophobic cavity. The inner width of the  $\beta$ -CD cavity is 6.0–6.5 Å and the height of one  $\beta$ -CD unit is 7.9 Å. From the structural point of view, the  $\beta$ -CD cavity is suitable to accommodate one carboxyl group and to bind with the pyridinium group. In this work, we aimed at developing photochromic materials with exceptional color changes by using  $\beta$ -CD and conjugation-extended viologens. Therefore, we designed and synthesized two conjugation-extended viologens, as shown in Fig. 1, one being *N,N'*-bis(4-carboxyphenyl)-(4,4'-bipyridinium) dichloride (viologen guest 2-Cl<sub>2</sub>) and the other one being *N,N'*-di(4-carboxyphenyl)-4,4'-(1,4-phenylene)-bipyridinium dichloride (viologen guest 3-Cl<sub>2</sub>; <sup>1</sup>H NMR and <sup>13</sup>C NMR spectra shown in Fig. S1, ESI†). For comparison, a traditional *N*-alkyl-substituted viologen, 1-(3-carboxybenzyl)-(4,4'-bipyridinium) dichloride (viologen guest 1-Cl<sub>2</sub>; <sup>1</sup>H NMR and <sup>13</sup>C NMR spectra shown in Fig. S2, ESI†), was also prepared. The binding behaviors of these three viologens with the  $\beta$ -CD in aqueous solution were investigated. It was found that the three viologens can be partly embedded into the  $\beta$ -CD to form supramolecular host-guest inclusion complexes. The solid-state samples of the formed inclusion complexes exhibit interesting bathochromic-shifted photochromism and photomodulable fluorescence. The distinct photochromic behaviors and fluorescence emissions of the inclusion complexes endow them with potential applications in many areas.

## Results and discussion

### Host-guest complexation between $\beta$ -CD and viologen guests

To investigate the host-guest complexation between  $\beta$ -CD and the three viologens, we used the NMR spectroscopic technique. The 2D gCOSY spectroscopy of the three viologens (Fig. S3, ESI†) was performed to assist the assignment of the <sup>1</sup>H NMR signals. Given that their <sup>1</sup>H NMR spectra (Fig. 2 and Fig. S4, S5, ESI†) display similar variation features, the viologen guest 3-Cl<sub>2</sub> is taken as an example to illustrate their binding interactions

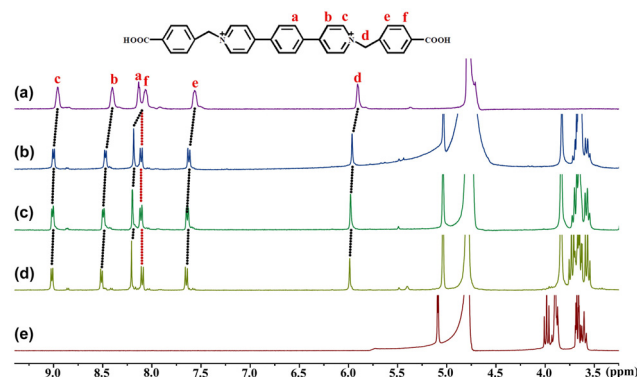
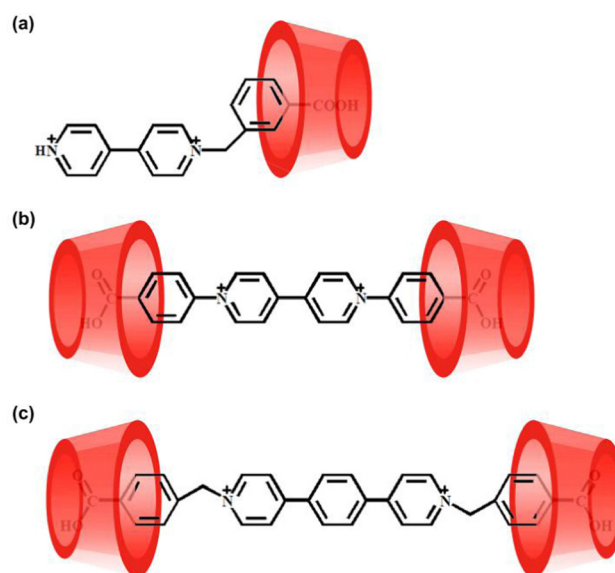


Fig. 2 <sup>1</sup>H NMR spectra (400 MHz, D<sub>2</sub>O) of the 3<sup>2+</sup> (4.0 mmol L<sup>−1</sup>, a) binding with (b) 0.52, (c) 1.13, and (d) 2.11 equiv. of  $\beta$ -CD in D<sub>2</sub>O at 20 °C. (e) The <sup>1</sup>H NMR spectrum (400 MHz, D<sub>2</sub>O) of  $\beta$ -CD in D<sub>2</sub>O (5.0 mmol L<sup>−1</sup>) at 20 °C.

with the  $\beta$ -CD. As shown in Fig. 2, in the presence of different concentrations of  $\beta$ -CD, all the protons of the guest 3<sup>2+</sup> are found to show downfield shift. This observation indicates that both the benzyl and the (1,4-phenylene)bipyridinium units of the guest 3<sup>2+</sup> are located outside of the  $\beta$ -CD portals, while the carboxy group of the guest 3<sup>2+</sup> was encapsulated into the  $\beta$ -CD cavity. In the presence of enough  $\beta$ -CD, they form a ternary 2 : 1 host-guest inclusion complex, 3<sup>2+</sup>@ $\beta$ -CD<sub>2</sub>, as illustrated in Scheme 1. The formation of the inclusion complex should be ascribed to the hydrophobic effect and van der Waals interaction between the  $\beta$ -CD and 3<sup>2+</sup>. Furthermore, only a single set of signals for 3<sup>2+</sup> were observed at different concentrations of  $\beta$ -CD, indicating that the guest exchange is fast compared to the NMR time scale. The binding models of the other two viologen guests with the  $\beta$ -CD are also illustrated in Scheme 1, suggesting that they form 1 : 1 and 2 : 1 host-guest inclusion complexes of 1<sup>2+</sup>@ $\beta$ -CD and 2<sup>2+</sup>@ $\beta$ -CD<sub>2</sub>. It must be noticed that



Scheme 1 Schematic view of the guests 1<sup>2+</sup> (a), 2<sup>2+</sup> (b), and 3<sup>2+</sup> (c) binding with the  $\beta$ -CD.





the detailed structures of these inclusion complexes are unclear because we fail to obtain their single crystals.

### Photochromic Properties of the inclusion complexes

The solid state of viologen guests  $1\text{-Cl}_2$ ,  $2\text{-Cl}_2$  and  $3\text{-Cl}_2$  exhibit very weak photochromism (Fig. S6, ESI<sup>†</sup>). In aqueous solution, no obvious photochromism was observed for the inclusion complexes  $1^{2+}@\beta\text{-CD}$ ,  $2^{2+}@\beta\text{-CD}_2$ , and  $3^{2+}@\beta\text{-CD}_2$  even under prolonged light irradiation (300 W xenon lamp). However, their solid-state samples display interesting photochromic behaviors. As shown in Fig. 3a, upon light irradiation, the inclusion complex  $1^{2+}@\beta\text{-CD}$  gradually changed from white to blue and tended to be saturated after 3 minutes of irradiation. After leaving in the dark at room temperature for about 8.0 hours, the blue photoproduct of the inclusion complex  $1^{2+}@\beta\text{-CD}$  returned to the initial white color. In addition, the discolored  $1^{2+}@\beta\text{-CD}$  can undergo color changes repeatedly as long as it is irradiated by light. In other words, the coloration and decoloration process of the inclusion complex  $1^{2+}@\beta\text{-CD}$  is reversible. For the inclusion complexes  $2^{2+}@\beta\text{-CD}_2$  (Fig. 3b) and  $3^{2+}@\beta\text{-CD}_2$  (Fig. 3c), by irradiating with a 300 W xenon lamp for about 3 minutes, their solid-state powder colors changed from pale yellow and white to green and orange, respectively. When the colored inclusion complexes were placed in the dark at room temperature, their colors gradually faded away and finally returned to the original pale yellow and white within 4.0 hours. Obviously, the color changes of the inclusion complexes  $2^{2+}@\beta\text{-CD}_2$  and  $3^{2+}@\beta\text{-CD}_2$  are also reversible. To be noted, although the surfaces of the samples for these inclusion complexes undergo color changes upon light irradiation, the inner parts

retain their original colors (Fig. S4, ESI<sup>†</sup>). Thus, these inclusion complexes have potential applications in the field of protection.

The color change processes of the three inclusion complexes were investigated by solid-state UV-vis diffuse-reflectance spectroscopy. As shown in Fig. 4a, before light irradiation all inclusion complexes show weak absorption in the visible and short-wave near-infrared regions (400–1250 nm). Upon light irradiation for about 3 minutes, two distinct absorption bands with centers at  $\sim 400$  nm and  $\sim 620$  nm appear for the inclusion complex  $1^{2+}@\beta\text{-CD}$ , which can be assigned to the  $\pi \rightarrow \pi^*$  electron transition of the photoproduct.<sup>60</sup> The solid-state UV-vis diffuse-reflectance spectra of the inclusion complexes  $2^{2+}@\beta\text{-CD}_2$  and  $3^{2+}@\beta\text{-CD}_2$  after light irradiation are totally different from that of  $1^{2+}@\beta\text{-CD}$ . Compared with the photochromic materials constructed using the traditional *N*-alkyl-substituted viologens, the absorption bands of the inclusion complexes  $2^{2+}@\beta\text{-CD}_2$  and  $3^{2+}@\beta\text{-CD}_2$  dramatically move to the longer wavelength region after light irradiation (Fig. 4b and c), which can be assigned to the  $n \rightarrow \pi^*$  electron transition.<sup>60</sup> In particular,  $3^{2+}@\beta\text{-CD}_2$  exhibited two characteristic absorption bands with centers at  $\sim 520$  nm and  $\sim 1000$  nm, and the latter belongs to the short-wave near-infrared region. Obviously, the strong bathochromic-shift of the absorption bands should be attributed to the increase of the  $\pi$ -conjugation length of the viologens in the inclusion complexes. Consequently, the inclusion complexes  $1^{2+}@\beta\text{-CD}$ ,  $2^{2+}@\beta\text{-CD}_2$  and  $3^{2+}@\beta\text{-CD}_2$  undergo obvious color changes from blue to green and then to orange. These results suggest that the colors of the photoproducts can be precisely controlled by tuning the effective  $\pi$ -conjugation length of the viologens.

Electron-spin resonance (ESR) spectra were also recorded to characterize these color change processes. The ESR profiles of the three inclusion complexes suggest that the photochromism is caused by a photo-induced electron-transfer chemical process. As can be seen from Fig. 5, all inclusion complexes are ESR silent before light irradiation but exhibit sharp resonance signals centered at  $g = 2.002$ ,  $g = 1.998$  and  $g = 1.999$ , respectively, after light irradiation. The  $g$  values are very close to that of a free electron ( $g = 2.0023$ ) observed in previously reported viologen-based complexes,<sup>21–26</sup> which confirms the generation of free radicals during the photochromic process. Therefore, the photochromic mechanism of these inclusion complexes is derived from the generation of free radicals, including normal viologen radicals ( $V^{\bullet+}$ ) and extended viologen radicals ( $\text{Ex}V^{\bullet+}$ ). To further understand the electron transfer process between the  $\beta\text{-CD}$  host and the viologen guests, DFT

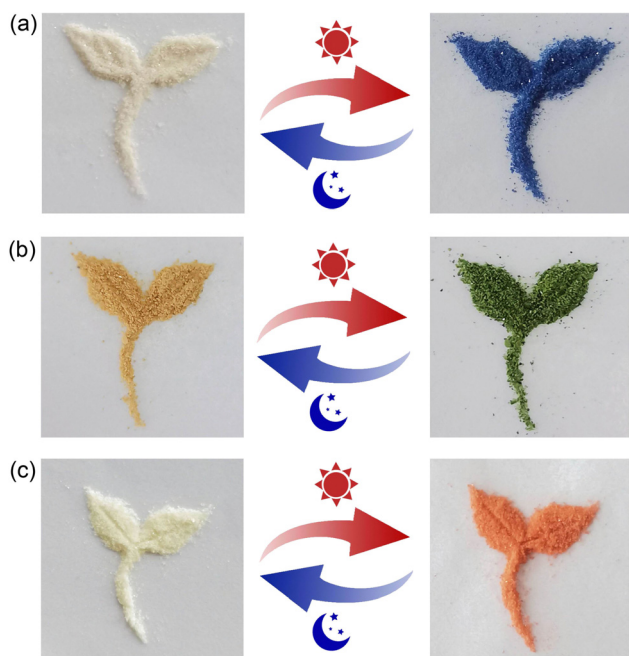


Fig. 3 Photographs showing the photochromic performances of the inclusion complexes  $1^{2+}@\beta\text{-CD}$  (a),  $2^{2+}@\beta\text{-CD}_2$  (b) and  $3^{2+}@\beta\text{-CD}_2$  (c) upon light irradiation with a xenon lamp.

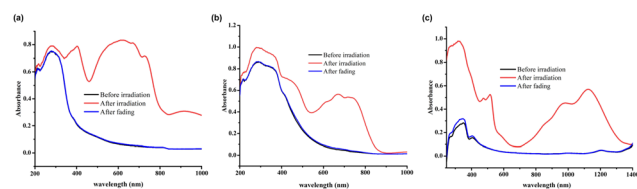


Fig. 4 UV-vis diffuse-reflectance spectra of the inclusion complexes  $1^{2+}@\beta\text{-CD}$  (a),  $2^{2+}@\beta\text{-CD}_2$  (b) and  $3^{2+}@\beta\text{-CD}_2$  (c) before and after light irradiation.





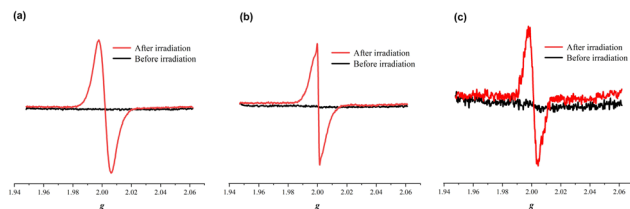


Fig. 5 ESR spectra of the inclusion complexes  $1^{2+}@β\text{-CD}$  (a),  $2^{2+}@β\text{-CD}$  (b) and  $3^{2+}@β\text{-CD}$  (c) before and after irradiation.

calculations were carried out for their 1 : 1 host-guest inclusion complexes. After obtaining their energy minimized structures in the gas phase, we calculated their highest occupied molecular orbitals (HOMOs) and lowest unoccupied molecular orbitals (LUMOs). It is found that the electron distribution of the HOMO is mainly located on the  $β\text{-CD}$  host, while that of the LUMO is mainly located on the pyridinium group of the viologen guests (Fig. S8–S10, ESI<sup>†</sup>). Such electron distributions on the HOMO and LUMO in the inclusion complexes reveal that the host  $β\text{-CD}$  acts as an electron donor, while the pyridinium unit in the viologen guests acts as an electron acceptor. The photochromic process of these inclusion complexes should be attributed to the photo-induced electron transfer from the host to the guest. In addition, we found that the FI-IR spectra of these three inclusion complexes (Fig. S11–S13, ESI<sup>†</sup>) are essentially identical before and after light irradiation. This observation suggests that there is no significant change in the geometric structure of these three inclusion complexes during the photochromic process.

### Photomodulable fluorescence

The fluorescence enhancement of a guest by complexation in a host has been thoroughly characterized by Kohler, Galoppini, Bhasikuttan, Nau and others.<sup>61–63</sup> We noticed that the fluorescence of the viologen guest  $3\text{-Cl}_2$  is green in the solid state. However, its inclusion complex with  $β\text{-CD}$  ( $3^{2+}@β\text{-CD}_2$ ) in the solid state emits brilliant pale-blue fluorescence under lab UV light ( $\lambda_{\text{ex}} = 365 \text{ nm}$ ). More interestingly, when the color of the inclusion complex  $3^{2+}@β\text{-CD}_2$  changed to orange after Xe-light irradiation, the fluorescence sharply declined (Fig. 6a). Hence, it is anticipated that the fluorescence intensity of the inclusion complex  $3^{2+}@β\text{-CD}_2$  can be modulated through the

photochromic process. As shown in Fig. 6b, the inclusion complex  $3^{2+}@β\text{-CD}_2$  shows a strong emission peak at 430 nm ( $\lambda_{\text{ex}} = 365 \text{ nm}$ ), which corresponds to the light blue fluorescence. When the photochromic process tented to saturate and the inclusion complex color completely changed to orange after Xe-light irradiation for 30 s, its fluorescence intensity was quenched by 87.2%. At the same time, its emission peak is slightly blue-shifted by about 10 nm. Obviously, the degree of fluorescence intensity reduction is dependent on the light irradiation time. It is generally agreed that the transformation from the emissive ligand/guest molecules to their corresponding nonemissive radical species leads to the fluorescence quenching. When the colored inclusion complex  $3^{2+}@β\text{-CD}_2$  returned to the initial color by long exposure to air, its fluorescence intensity was entirely recovered. Obviously, the reversible fluorescence “on–off” switching process is controlled by the photochromic process.

The fluorescence spectra of the inclusion complexes  $1^{2+}@β\text{-CD}$  and  $2^{2+}@β\text{-CD}_2$  were also measured during the photochromic process. We observed that their fluorescence intensities are much smaller than that of  $3^{2+}@β\text{-CD}_2$ . Upon excitation at 365 nm, the inclusion complex  $1^{2+}@β\text{-CD}$  emitted a light green fluorescence and showed a single peak at 450 nm (Fig. S14, ESI<sup>†</sup>). When the photochromic process of  $1^{2+}@β\text{-CD}$  became saturated, its fluorescence quenching efficiency reached 94.2%. In the case of  $2^{2+}@β\text{-CD}_2$ , it shows a light yellow fluorescence with an emission peak at 520 nm. After light irradiation for 3 minutes, its emission is quenched by 87.0% (Fig. S15, ESI<sup>†</sup>).

### Applications in inkless printing, anti-counterfeiting and encryption

It is well known that photochromic materials can be used for erasable inkless printing and anti-counterfeiting in addition to the protection application discussed above. However, the often encountered problem is the limited colors of photoproducts. Due to the different  $\pi$ -conjugation lengths of the viologens  $1\text{-Cl}_2$ ,  $2\text{-Cl}_2$  and  $3\text{-Cl}_2$ , the photoproducts of the corresponding  $β\text{-CD}$  inclusion complexes display three completely different colors, including blue, green and orange, which makes multi-color inkless printing possible. Different inclusion complexes were first coated onto different filter papers by using a previously reported method.<sup>10,22,64,65</sup> The prepared filter paper was then covered with a mask and irradiated with a xenon lamp. Removing the mask, the target pattern was successfully printed on the filter paper, as can be seen from Fig. 7a. The printed patterns gradually disappeared in an hour. Naturally, the prepared filter papers can be repeatedly printed with other patterns.

The combination of different photochromic materials can significantly enhance the level of anti-counterfeiting technology. Here we prepared a specific filter paper, different areas of which were coated with different inclusion complexes. Using the same method mentioned above, we obtained a colorful two-dimensional code (Quick Response code, QR code) on the prepared filter paper and successfully decoded it on a smartphone installed with the corresponding APP software

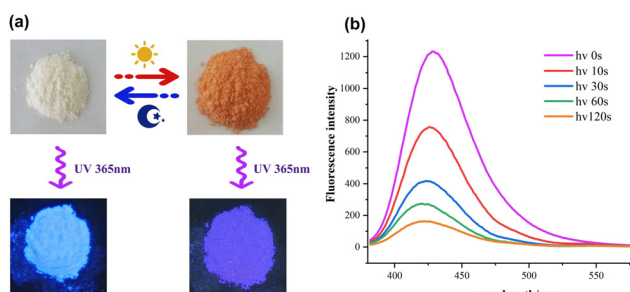


Fig. 6 (a) Photographs showing the fluorescence emissions of the solid-state  $3^{2+}@β\text{-CD}_2$  before and after irradiation. (b) Fluorescence spectra of the solid-state  $3^{2+}@β\text{-CD}_2$  under different light irradiation times.





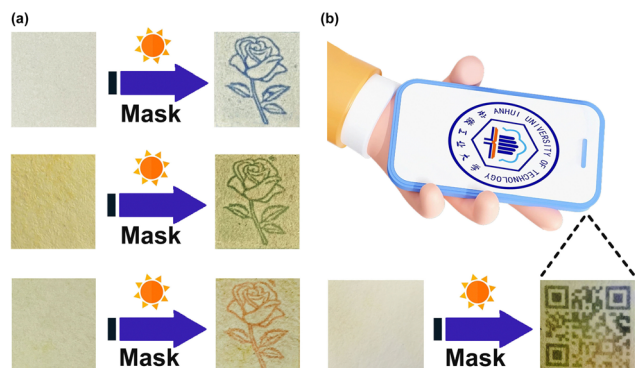


Fig. 7 (a) Erasable inkless printing on the filter papers coated with the three inclusion complexes. (b) The QR code "printed" on a specific filter paper can be recognized by a smartphone.

(Fig. 7b). Making the QR code with different photochromic materials will enhance the anti-counterfeiting capabilities.

In addition, the different photochromic behaviors and fluorescence emissions of the three inclusion complexes endow them with the capability of constructing multilevel encryption information. As demonstrated in Fig. 8, the three inclusion complexes were coated on three fan-shaped filter papers, respectively. At the same time, three different colors were labeled with three different numbers. Blue was labeled as "1", green was labeled as "2", and orange was labeled as "3". Upon exposure to light irradiation, the colors of the three fan-shaped filter papers will change to display the encryption information. According to the predesigned code book 1 (Table S1, ESI<sup>†</sup>), the correct message can be decoded. In the same way, three different fluorescence emissions were also labeled with three different numbers. Light green fluorescence was labeled as "1", light yellow was labeled as "2", and light blue was labeled as "3". Under lab UV light ( $\lambda_{\text{ex}} = 365 \text{ nm}$ ), the three fan-shaped filter papers emitted different fluorescence emissions. Using the predesigned code book 2 (Table S2, ESI<sup>†</sup>), we can obtain the correct message. In this information encryption system, obtaining the correct information requires knowing not only the correct code book, but also the correct light irradiation, under UV light or Xe-light.

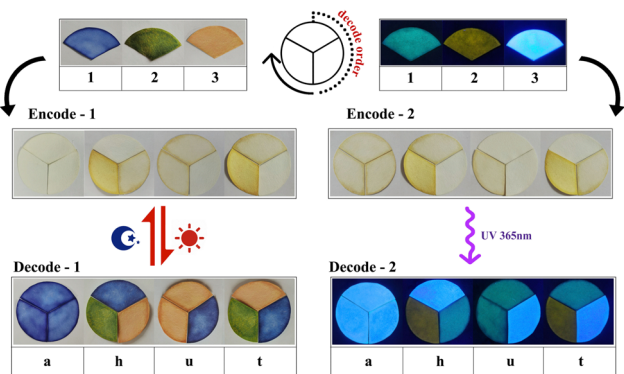


Fig. 8 Schematic illustrations showing the application of the three inclusion complexes in information encryption.

## Experimental

### Materials

Starting materials for syntheses and the macrocyclic host  $\beta$ -CD were purchased from Sigma-Aldrich and Aladdin and used as received without further purification.

### Synthesis

Synthesis of 1-(3-carboxybenzyl)-(4,4'-bipyridinium) dichloride (guest 1-Cl<sub>2</sub>): 4,4'-bipyridine (0.5 g, 0.0032 mol) and 3-chloromethyl-benzoic acid (0.49 g, 0.0029 mol) were dissolved in AcCN (25 mL). In the oil bath, the solution was heated to 80 °C and refluxed for 12 h. The precipitate was filtered and washed with ethanol. Then the precipitate was treated with dilute hydrochloric acid solution to give viologen guest 1-Cl<sub>2</sub> (0.22 g, 28%). M.p.: 273–275 °C. FT-IR (KBr, cm<sup>-1</sup>): 3415 (m), 3042 (m), 1710 (s), 1635 (s), 1596 (m), 1557 (w), 1504 (w), 1457 (m), 1370 (w), 1290 (m), 1238 (w), 1194 (m), 1112 (w), 1002 (w), 818 (w), 789 (w), 740 (w), 691 (w), 651 (w), and 564 (w).

<sup>1</sup>H NMR (400 MHz, D<sub>2</sub>O)  $\delta$  9.10 (dd,  $J = 28.5, 6.4 \text{ Hz}$ , 7H), 9.05 (s, 1H), 8.85 (t,  $J = 6.8 \text{ Hz}$ , 6H), 8.46 (dd,  $J = 26.6, 6.6 \text{ Hz}$ , 8H), 8.23 (d,  $J = 6.6 \text{ Hz}$ , 3H), 8.14 (d,  $J = 6.5 \text{ Hz}$ , 3H), 7.99 (d,  $J = 7.1 \text{ Hz}$ , 7H), 7.67 (d,  $J = 7.7 \text{ Hz}$ , 4H), 7.56 (t,  $J = 7.5 \text{ Hz}$ , 3H), 5.93 (d,  $J = 11.4 \text{ Hz}$ , 7H), 4.79 (s, 35H), 2.01 (s, 1H). <sup>13</sup>C NMR (101 MHz, D<sub>2</sub>O)  $\delta$  171.37 (s), 150.35 (s), 146.67 (s), 145.60 (s), 145.01 (d,  $J = 33.9 \text{ Hz}$ ), 133.68 (s), 133.15 (d,  $J = 5.8 \text{ Hz}$ ), 132.80 (s), 132.55 (s), 130.76 (d,  $J = 6.4 \text{ Hz}$ ), 129.83 (d,  $J = 7.3 \text{ Hz}$ ), 127.23 (s), 126.67 (s), 124.66 (s), 124.16 (s), 64.35 (s), 64.03 (s). HRMS (ESI)  $m/z$  [1-H]<sup>+</sup> calcd for C<sub>18</sub>H<sub>15</sub>N<sub>2</sub>O<sub>2</sub><sup>+</sup> 291.1120, found 291.1117.

### Synthesis of *N,N'*-bis(4-carboxyphenyl)-(4,4'-bipyridinium) dichloride (guest 2-Cl<sub>2</sub>)

Guest 2-Cl<sub>2</sub> was synthesized according to the procedures reported in the literature.

### Synthesis of *N,N'*-di(4-carboxyphenyl)-4,4'-(1,4-phenylene)-bipyridinium dichloride (guest 3-Cl<sub>2</sub>)

A solution of 1,4-bis(pyrid-4-yl)benzene (0.3 g, 0.0013 mol) and 4-chloromethyl-benzoic acid (0.5 g, 0.003 mol) in DMF (20 mL) was refluxed for 12 h. After cooling, the faint yellow product formed was collected by filtration, washed with ethanol, and then dried *in vacuo* to give 3-Cl<sub>2</sub> as a faint yellow powder. Yield: 74% based on 1,4-bis(pyrid-4-yl)benzene. M.p.: 320–325 °C. FT-IR (KBr, cm<sup>-1</sup>): 3425 (m), 3034 (m), 1713 (s), 1634 (s), 1562 (w), 1538 (w), 1495 (m), 1471 (m), 1390 (m), 1277 (m), 1230 (m), 1165 (m), 1115 (w), 1021 (w), 882 (w), 814 (m), 780 (m), 749 (m), 704 (w), 631 (w), 571 (w), 517 (w). <sup>1</sup>H NMR (400 MHz, D<sub>2</sub>O)  $\delta$  8.96 (s, 9H), 8.40 (s, 10H), 8.13 (s, 8H), 8.07 (s, 8H), 7.92 (s, 2H), 7.56 (s, 9H), 5.91 (s, 9H), 4.79 (d,  $J = 3.9 \text{ Hz}$ , 208H). <sup>13</sup>C NMR (101 MHz, DMSO)  $\delta$  145.74 (s), 130.51 (s), 129.86 (s), 129.36 (s), 126.00 (s), 40.59 (s), 40.28 (d,  $J = 21.0 \text{ Hz}$ ), 40.17 (s), 40.07 (d,  $J = 21.0 \text{ Hz}$ ), 39.76 (s), 39.61 (s), 39.44 (d,  $J = 21.0 \text{ Hz}$ ). HRMS (ESI)  $m/z$  [3-H]<sup>+</sup> calcd for C<sub>32</sub>H<sub>25</sub>N<sub>2</sub>O<sub>4</sub><sup>+</sup> 501.1832, found 501.1788.





## General

$^1\text{H}$  NMR,  $^{13}\text{C}$  NMR, and 2D gCOSY NMR spectra were recorded on a Bruker DPX 400 spectrometer at 293.15 K. The solid samples are added directly into NMR tubes. HRMS was carried out on an Agilent 6540 Q-TOF mass spectrometer (Agilent Technologies, Inc., Santa Clara, CA). Solid-state UV-vis spectra were recorded on a Shimadzu UV3600 ultraviolet-visible spectrophotometer equipped with an integrating sphere in the wavelength range of 200–800 nm. A  $\text{BaSO}_4$  plate was used as a reference (100% reflectance), on which the finely ground powders of the samples were coated. Electron-spin resonance (ESR) spectra were recorded on a Bruker A300 spectrometer with a 100 kHz magnetic field in the X band at room temperature. FT-IR spectra were obtained with a Nicolet Magna 750 spectrometer using KBr disks in the range of 3000–400  $\text{cm}^{-1}$ . Photochromic tests were performed using a 300 W xenon lamp system (CEL-HXF300, 1000  $\text{W m}^{-2}$ ), with the samples being placed at 50 cm from the lamp. The fluorescence spectra of the solid-state samples were recorded at 25  $^\circ\text{C}$  using a Varian Cary Eclipse spectrofluorometer (Varian, Inc., Palo Alto, CA, USA).

## DFT calculations

Geometry optimizations were carried out using Gaussian-03 software.<sup>66</sup> The DFT geometry optimizations of the inclusion complexes were performed using a B3LYP/6-311G(d,p) basis set. The frontier molecular orbital properties of the inclusion complexes were calculated using HOMO–LUMO orbitals. HOMO–LUMO orbital analysis was used to determine intramolecular electron transfer.

## Preparation of the solid-state samples of the inclusion complexes $1^{2+}$ @ $\beta$ -CD, $2^{2+}$ @ $\beta$ -CD<sub>2</sub> and $3^{2+}$ @ $\beta$ -CD<sub>2</sub>

$\beta$ -CD (0.18 g, 0.16 mmol) and guest 1-Cl<sub>2</sub> (0.05 g, 0.14 mmol) were dissolved in 10 mL water. The solvent water was removed by vacuum-rotary evaporation. The solid product of  $1^{2+}$ @ $\beta$ -CD was obtained after drying under vacuum. The solid-state samples of the other two inclusion complexes were prepared according to the same procedure.

## Conclusions

In summary, three viologen derivatives, one being traditional *N*-alkyl-substituted viologen and the other two being conjugation-extended viologens, have been designed and synthesized. NMR spectroscopy analysis has revealed that these three viologen guests can bind with the  $\beta$ -CD host to form 1:1 or 2:1 host–guest inclusion complexes in aqueous solution. The formed inclusion complexes in the solid state exhibit bathochromic-shifted photochromic behaviors, and the colors of their photoproducts are blue, green and orange, respectively. The ESR spectra and DFT calculations of the inclusion complexes indicate that the observed photochromism is caused by the photo-induced electron transfer from the  $\beta$ -CD host to the viologen guests, which results in the generation of free radicals. On the other hand, it is found that the three inclusion complexes show fluorescence emissions, while

their photoproducts are fluorescence-quenched, suggesting that the fluorescence intensity is modulated by the photochromic processes. By using the photochromic and fluorescence properties of the three inclusion complexes, we have also demonstrated their applications in protection, erasable inkless multi-color printing, multiple anti-counterfeiting and multilevel information encryption. Overall, this work provides an effective path to tune the photochromic properties of the viologen derivatives encapsulated in the macrocycle. Photochromic materials with new color variations will find wider applications in the future.

## Author contributions

D.-X. Xia and L.-W. Fan performed the experiments. W.-Q. Sun performed the DFT calculations. M.-F. Ye, R.-L. Lin and J.-X. Liu conceived and directed the project and wrote the paper. All authors discussed the results and commented on the manuscript.

## Conflicts of interest

There are no conflicts to declare.

## Acknowledgements

This work was supported by the National Natural Science Foundation of China (Grant No. 21371004), the Natural Science Foundation of Anhui Province (2008085MB36), and the Natural Science Research Project of Anhui Province Education Department (2023AH040150 and 2023AH051116).

## Notes and references

- 1 H. Bouas-Laurent and H. Durr, Organic photochromism (IUPAC technical report), *Pure Appl. Chem.*, 2001, **73**, 639–665.
- 2 H. Tian and J. Zhang, *Photochromic Materials: Preparation, Properties and Applications*, Wiley-VCH, Weinheim, Germany, 2016.
- 3 C.-C. Ko and V. W.-W. Yam, Coordination Compounds with Photochromic Ligands: Ready Tunability and Visible Light-Sensitized Photochromism, *Acc. Chem. Res.*, 2018, **51**, 149–159.
- 4 D.-D. Yang, Y.-S. Shi, T. Xiao, Y.-H. Fang and X.-J. Zheng, Three-Dimensional Viologen-Based Lanthanide-Organic Frameworks: Photochromism and Fluorescence Detection of Quinolone Antibiotics, *Inorg. Chem.*, 2023, **62**, 6084–6091.
- 5 S.-L. Li, K.-J. Li, Y. Shen, Y.-J. Wang, W. Yang, M. Qu, Z. Qi, J. Zhang and X.-M. Zhang, Selective Photochromic Response to Low-Dose X-ray Radiation Detection in One-Dimensional Cadmium-Viologen Complexes, *Inorg. Chem.*, 2023, **62**, 4990–4998.
- 6 Y. Fu, H. Zhao, Y. Wang, D. Chen, Z. Yu, J. Zheng, S. Sun, W. Cai and H. Zhou, Reversible Photochromic Photonic





- Crystal Device With Dual Structural Colors, *ACS Appl. Mater. Interfaces*, 2022, **14**, 29070–29076.
- 7 M. Irie, T. Fukaminato, K. Matsuda and S. Kobatake, Photochromism of aryethene Molecules and Crystals: Memories, Switches, and Actuators, *Chem. Rev.*, 2014, **114**, 12174–12277.
  - 8 W. An, D. Aulakh, X. Zhang, W. Verdegaal, K. R. Dunbar and M. Wriedt, Switching of Adsorption Properties in a Zwitterionic Metal–Organic Framework Triggered by Photo-generated Radical Triplets, *Chem. Mater.*, 2016, **28**, 7825–7832.
  - 9 T. Zhou, J. Chen, T. Wang, H. Yan, Y. Xu, Y. Li and W. Sun, One-Dimensional Chain Viologen-Based Lanthanide Multistimulus-Responsive Materials with Photochromism, Photoluminescence, Photomagnetism, and Ammonia/Amine Vapor Sensing, *ACS Appl. Mater. Interfaces*, 2022, **14**, 57037–57046.
  - 10 B. Garai, A. Mallick and R. Banerjee, Photochromic Metal–Organic Frameworks for Inkless and Erasable Printing, *Chem. Sci.*, 2016, **7**, 2195–2200.
  - 11 H. Zhang and X. T. Wu, Calix-Like Metal–Organic Complex for High-Sensitivity X-Ray-Induced Photochromism, *Adv. Sci.*, 2016, **3**, 1500224.
  - 12 T. Gong, X. Yang, J.-J. Fang, Q. Sui, F.-G. Xi and E.-Q. Gao, Distinct Chromic and Magnetic Properties of Metal–Organic Frameworks with a Redox Ligand, *ACS Appl. Mater. Interfaces*, 2017, **9**, 5503–5512.
  - 13 P. X. Li, M. S. Wang, M. J. Zhang, C. S. Lin, L. Z. Cai, S. P. Guo and G. C. Guo, Electron-Transfer Photochromism to Switch Bulk Second-Order Nonlinear Optical Properties with High Contrast, *Angew. Chem., Int. Ed.*, 2014, **53**, 11529–11531.
  - 14 T. Gong, P. Li, Q. Sui, L. J. Zhou, N. N. Yang and E. Q. Gao, Switchable Ferro-, Ferri-, and Antiferromagnetic States in a Piezo- and Hydrochromic Metal–Organic Framework, *Inorg. Chem.*, 2018, **57**, 6791–6794.
  - 15 Q. Shi, S.-Y. Wu, X.-T. Qiu, Y.-Q. Sun and S.-T. Zheng, Three viologen-derived Zn-organic materials: photochromism, photomodulated fluorescence, and inkless and erasable prints, *Dalton Trans.*, 2019, **48**, 954–963.
  - 16 H. Lu, H. Huang, J. Yang, Z. Zheng, X. Dong, L. Zhao, C. Xu, J. Hu, H. Liu, Y. Qian, J.-Q. Wang and J. Lin, Incorporating Photochromic Viologen Derivative to Unprecedentedly Boost UV Sensitivity in Photoelectrochromic Hydrogel, *ACS Sens.*, 2023, **8**, 1609–1615.
  - 17 C. Chen, J. K. Sun, Y. J. Zhang, X. D. Yang and J. Zhang, Flexible Viologen-Based Porous Framework Showing X-ray Induced Photochromism with Single-Crystal-to-Single-Crystal Transformation, *Angew. Chem., Int. Ed.*, 2017, **56**, 14458–14462.
  - 18 Q. Sui, P. Li, N. N. Yang, T. Gong, R. Bu and E. Q. Gao, Differentiable Detection of Volatile Amines with a Viologen-Derived Metal–Organic Material, *ACS Appl. Mater. Interfaces*, 2018, **10**, 11056–11062.
  - 19 T. M. Bockman and J. K. Kochi, Isolation and Oxidation-Reduction of Methylviologen Cation Radicals. Novel Disproportionation in Charge-Transfer Salts by X-ray Crystallography, *J. Org. Chem.*, 1990, **55**, 4127–4135.
  - 20 N. Mercier, The templating effect and photochemistry of viologens in halometalate hydrid crystals, *Eur. J. Inorg. Chem.*, 2013, 19–31.
  - 21 S. Hu, J. Zhang, Y. He, Z. Chen and Z. Fu, A *N*-Aromatic-Substituted Viologen-Based Coordination Polymer with Layered Assembly of Hydrogen-Bonded Networks Showing Exceptional Photochromic Behaviors, *Cryst. Growth Des.*, 2019, **19**, 543–546.
  - 22 C.-M. Yu, P.-H. Wang, Q. Liu, L.-Z. Cai and G.-C. Guo, Modulating Fading Time of Photochromic Compounds by Molecular Design for Erasable Inkless Printing and Anti-counterfeiting, *Cryst. Growth Des.*, 2021, **21**, 1323–1328.
  - 23 P.-Y. Guo, C. Sun, N.-N. Zhang, L.-Z. Cai, M.-S. Wang and G.-C. Guo, An inorganic–organic hybrid photochromic material with fast response to hard and soft X-rays at room temperature, *Chem. Commun.*, 2018, **54**, 4525–4528.
  - 24 S.-L. Li, M. Han, Y. Zhang, G.-P. Li, M. Li, G. He and X.-M. Zhang, X-ray and UV Dual Photochromism, Thermochromism, Electrochromism, and Amine-Selective Chemochromism in an Anderson-like Zn<sub>7</sub> Cluster-Based 7-Fold Interpenetrated Framework, *J. Am. Chem. Soc.*, 2019, **141**, 12663–12672.
  - 25 X. D. Yang, L. Sun, C. Chen, Y. J. Zhang and J. Zhang, Anioncontrolled photochromism of two bipyridinium-based coordination polymers and nondestructive luminescence readout, *Dalton Trans.*, 2017, **46**, 4366–4372.
  - 26 Y. B. Su, Y. Q. Wei, L. Z. Cai, P. X. Li, M. S. Wang and G. C. Guo, Energy- dependent photochromism at room temperature for visually detecting and distinguishing X- rays, *Chem. Commun.*, 2018, **54**, 12349–12352.
  - 27 T. Gong, X. Yang, J. J. Fang, Q. Sui, F. G. Xi and E. Q. Gao, Distinct Chromic and Magnetic Properties of Metal–Organic Frameworks with a Redox Ligand, *ACS Appl. Mater. Interfaces*, 2017, **9**, 5503–5512.
  - 28 J. Wang, S. L. Li and X. M. Zhang, Photochromic and Nonphotochromic Luminescent Supramolecular Isomers Based on Carboxylate-Functionalized Bipyridinium Ligand: (4,4)-Net versus Interpenetrated (6,3)-Net, *ACS Appl. Mater. Interfaces*, 2016, **8**, 24862–24869.
  - 29 S.-L. Li, M. Han, B. Wu, J. Wang and X.-M. Zhang, Photochromic Porous and Nonporous Viologen-Based Metal–Organic Frameworks for Visually Detecting Oxygen, *Cryst. Growth Des.*, 2018, **18**, 3883–3889.
  - 30 R.-G. Lin, G. Xu, G. Lu, M.-S. Wang, P.-X. Li and G.-C. Guo, Photochromic Hybrid Containing in situ Generated Benzyl Viologen and Novel Trinuclear [Bi<sub>3</sub>Cl<sub>14</sub>]<sub>5</sub><sup>−</sup>: Improved Photoresponsibility by the  $\pi \cdots \pi$  Interactions and Size Effect of Inorganic Oligomer, *Inorg. Chem.*, 2014, **53**, 5538–5545.
  - 31 R.-G. Lin, G. Xu, M.-S. Wang, G. Lu, P.-X. Li and G.-C. Guo, Improved Photochromic Properties on Viologen-Based Inorganic–Organic Hybrids by Using  $\pi$ -Conjugated Substituents as Electron Donors and Stabilizers, *Inorg. Chem.*, 2013, **52**, 1199–1205.
  - 32 M.-S. Wang, C. Yang, G.-E. Wang, G. Xu, X.-Y. Lv, Z.-N. Xu, R.-G. Lin, L.-Z. Cai and G.-C. Guo, A Room-Temperature X-ray-Induced Photochromic Material for X-ray Detection, *Angew. Chem., Int. Ed.*, 2012, **51**, 3432–3435.





- 33 P.-X. Li, M.-S. Wang, L.-Z. Cai, G.-E. Wang and G.-C. Guo, Rare electron-transfer photochromic and thermochromic difunctional compounds, *J. Mater. Chem. C*, 2015, **3**, 253–256.
- 34 J.-K. Sun and J. Zhang, Functional metal–bipyridinium frameworks: self-assembly and applications, *Dalton Trans.*, 2015, **44**, 19041–19055.
- 35 M. Nanasawa, M. Miwa, M. Hirai and T. Kuwabara, Synthesis of Viologens with Extended  $\pi$ -Conjugation and Their Photochromic Behavior on Near-IR Absorption, *J. Org. Chem.*, 2000, **65**, 593–595.
- 36 M. Chang, W. Chen, H. Xue, D. Liang, X. Lu and G. Zhou, Conjugation-Extended Viologens with Thiophene Derivative Bridges: Near-infrared Electrochromism, Electrofluorochromism, and Smart Window Applications, *J. Mater. Chem. C*, 2020, **8**, 16129–16142.
- 37 M. Chang, D. Liang, F. Zhou, H. Xue, H. Zong, W. Chen and G. Zhou, Photochromic and Electrochromic Hydrogels Based on Ammonium and Sulfonate-Functionalized Thienoviologen Derivatives, *ACS Appl. Mater. Interfaces*, 2022, **14**, 15448–15460.
- 38 P. Li, L.-J. Zhou, N.-N. Yang, Q. Sui, T. Gong and E.-Q. Gao, Metal-Organic Frameworks with Extended Viologen Units: Metal-Dependent Photochromism, Photomodulable Fluorescence, and Sensing Properties, *Cryst. Growth Des.*, 2018, **18**, 7191–7198.
- 39 P. Li, M.-Y. Guo, X.-M. Yin, L.-L. Gao, S.-L. Yang, R. Bu, T. Gong and E.-Q. Gao, Interpenetration-Enabled Photochromism and Fluorescence Photomodulation in a Metal–Organic Framework with the Thiazolothiazole Extended Viologen Fluorophore, *Inorg. Chem.*, 2019, **58**, 14167–14174.
- 40 G. K. Pande, J. S. Heo, J. H. Choi, Y. S. Eom, J. Kim, S. K. Park and J. S. Park, RGB-to-Black Multicolor Electrochromic Devices Enabled with Viologen Functionalized Polyhedral Oligomeric Silsesquioxanes, *Chem. Eng. J.*, 2021, **420**, 130446.
- 41 A. Beneduci, S. Cospito, M. L. Deda and G. Chidichimo, Highly Fluorescent Thienoviologen-Based Polymer Gels for Single Layer Electrofluorochromic Devices, *Adv. Funct. Mater.*, 2015, **25**, 1240–1247.
- 42 G. A. Corrente, E. Fabiano, M. L. Deda, F. Manni, G. Gigli, G. Chidichimo, A. L. Capodilupo and A. Beneduci, High-Performance Electrofluorochromic Switching Devices Using a Novel Arylamine-Fluorene Redox-Active Fluorophore, *ACS Appl. Mater. Interfaces*, 2019, **11**, 12202–12208.
- 43 S. Seo, Y. Kim, Q. Zhou, G. Clavier, P. Audebert and E. Kim, White Electrofluorescence Switching from Electrochemically Convertible Yellow Fluorescent Dyad, *Adv. Funct. Mater.*, 2012, **22**, 3556–3561.
- 44 A. Heckmann and C. Lambert, Organic Mixed-Valence Compounds: A Playground for Electrons and Holes, *Angew. Chem., Int. Ed.*, 2012, **51**, 326–392.
- 45 A. Beneduci, S. Cospito, M. L. Deda, L. Veltri and G. Chidichimo, Electrofluorochromism in  $\pi$ -conjugated ionic liquid crystals, *Nat. Commun.*, 2014, **5**, 3105.
- 46 S. Cospito, A. Beneduci, L. Veltri, M. Salamoneczyk and G. Chidichimo, Mesomorphism and electrochemistry of thienoviologen liquid crystals, *Phys. Chem. Chem. Phys.*, 2015, **17**, 17670–17678.
- 47 A. Beneduci, S. Cospito, M. L. Deda and G. Chidichimo, Highly Fluorescent Thienoviologen-Based Polymer Gels for Single Layer Electrofluorochromic Devices, *Adv. Funct. Mater.*, 2015, **25**, 1240–1247.
- 48 Y.-W. Wang, M.-H. Li, S.-Q. Zhang, X. Fang and M.-J. Lin, A Three-Component Donor–Acceptor Hybrid Framework with Low-Power X-ray-Induced Photochromism, *Inorg. Chem.*, 2022, **61**, 8153–8159.
- 49 D. Luo, L.-Y. Guang, R.-G. Lin, N.-N. Zhang, M.-C. Liu, R. L. Lin, W.-Q. Sun and J. X. Liu, Chromic properties of carboxyphenyl viologen induced by complexation in cucurbit[7]uril, *ChemistrySelect*, 2021, **6**, 1699–1704.
- 50 Q. Wang, M. C. Liu, W. Q. Sun, R. L. Lin and J. X. Liu, Electron transfer photochromism of solid-state supramolecules between 1-(4-carboxybenzyl)-4-[2-(4-pyridyl)-vinyl] - pyridinium chloride and cucurbit[n]uril ( $n = 5-8$ ), *New J. Chem.*, 2021, **45**, 22249–22254.
- 51 Q. Wang, M. C. Liu, W. Q. Sun, R. L. Lin, R. G. Lin and J. X. Liu, Solid-State supramolecular inclusion complexes of  $\beta$ -cyclodextrin with carboxyphenyl viologens showing photochromic properties, *J. Phys. Chem. C*, 2022, **126**, 844–850.
- 52 Q. Wang, J. Z. Guo, C. Zhang, W. Q. Sun, R. L. Lin, M. F. Ye and J. X. Liu, Inclusion complexes of cyclodextrins with 1-(4-carboxybenzyl)-4-[2-(4-pyridyl)-vinyl]-pyridinium chloride: photochromism, erasable inkless printing and color tuning, *J. Phys. Chem. C*, 2022, **126**, 18900–18906.
- 53 Q. Wang, J. Z. Guo, D. Luo, M. F. Ye, R. L. Lin, W. Q. Sun and J. X. Liu, An Inclusion Complex of Cucurbit[7]uril with Benzimidazolyl Benzyl Viologen Showing Fluorescence and Photochromic Properties, *Phys. Chem. Chem. Phys.*, 2022, **24**, 25930–25936.
- 54 Q. Wang, X.-F. Wang, W.-Q. Sun, R.-L. Lin, M.-F. Ye and J.-X. Liu, A Supramolecular Host-Guest Hydrogel Based on  $\gamma$ -Cyclodextrin and Carboxybenzyl Viologen Showing Reversible Photochromism and Photomodulable Fluorescence, *ACS Appl. Mater. Interfaces*, 2023, **15**, 2479–2485.
- 55 H. Nie, Y. Rao, J. Song and X.-L. Ni, Through-Space Conjugated Supramolecular Polymer Radicals from Spatial Organization of Cucurbit[8]uril: An Efficient Approach for Electron Transfer and Smart Photochromism Materials, *Chem. Mater.*, 2022, **34**, 8925–8934.
- 56 J. Szejtli, Introduction and general overview of cyclodextrin chemistry, *Chem. Rev.*, 1998, **98**, 1743–1754.
- 57 T. S. Valerian and B. L. Kermey, Cyclodextrins: introduction, *Chem. Rev.*, 1998, **98**, 1741–1742.
- 58 Q. D. Hu, G. P. Tang and P. K. Chu, Cyclodextrin-based hostguest supramolecular nanoparticles for delivery: From design to applications, *Acc. Chem. Res.*, 2014, **47**, 2017–2025.
- 59 G. Crini, Review: A history of cyclodextrin, *Chem. Rev.*, 2014, **114**, 10940–10975.
- 60 K. Takahashi, T. Nihira, K. Akiyama, Y. Ikegami and E. Fukuyoc, Synthesis and Characterization of New





- Conjugation-Extended Viologens Involving A Central Aromatic Linking Group, *J. Chem. Soc., Chem. Commun.*, 1992, 620–622.
- 61 J. Peon, X. Tan, J. D. Hoerner, C. Xia, Y. F. Luk and B. Kohler, Excited State Dynamics of Methyl Viologen. Ultrafast Photoreduction in Methanol and Fluorescence in Acetonitrile, *J. Phys. Chem. A*, 2001, **105**, 5768–5777.
  - 62 A. C. Bhasikuttan, J. Mohanty, W. M. Nau and H. Pal, Efficient fluorescence enhancement and cooperative binding of an organic dye in a supra-biomolecular host-protein assembly, *Angew. Chem., Int. Ed.*, 2007, **46**, 4120–4122.
  - 63 M. Freitag, L. Gundlach, P. Piotrowiak and E. Galoppini, Fluorescence Enhancement of Di-p-tolyl Viologen by Complexation in Cucurbit[7]uril, *J. Am. Chem. Soc.*, 2012, **134**, 3358–3366.
  - 64 W.-Q. Kan, S.-Z. Wen, Y.-C. He and C.-Y. Xu, Viologen-Based Photochromic Coordination Polymers for Inkless and Erasable Prints, *Inorg. Chem.*, 2017, **56**, 14926–14935.
  - 65 D.-D. Yang, H.-W. Zheng, Y.-H. Fang, Q.-F. Liang, Q.-Z. Han, Y.-S. Shi and X.-J. Zheng, Multistimuli-Responsive Materials Based on Zn(II)-Viologen Coordination Polymers and Their Applications in Inkless Print and Anticounterfeiting, *Inorg. Chem.*, 2022, **61**, 7513–7522.
  - 66 M. J. Frisch, G. W. Trucks, H. B. Schlegel and G. E. Scuseria, *et al.*, *Gaussian 03 (Revision B.01)*, Gaussian, Inc., Pittsburgh PA, 2003.

